Hindawi Publishing Corporation
Journal of Nanomaterials
Volume 2011, Article ID 853832, 9 pages
doi:10.1155/2011/853832

Research Article

Facile Synthesis of Monodisperse ZnO Nanocrystals by Direct Liquid Phase Precipitation

Lan Chen, Justin D. Holmes, Sonia Ramírez-García, and Michael A. Morris

Department of Chemistry, University College Cork, Cork, Ireland

Correspondence should be addressed to Michael A. Morris, m.morris@ucc.ie

Received 21 May 2010; Accepted 6 July 2010

Academic Editor: Quanqin Dai

ZnO nanocrystals can be synthesized by a variety of methods. Among them, only a few nonhydrolytic methods have been successful at low synthesis temperatures in terms of size, crystallinity, morphology and surface-defect control. These methods require very careful control of conditions and carefully engineered precursors. A new methodology—*direct liquid phase precipitation*—is reported here that can produce nanocrystals (NCs) which are a little difficult to obtain for these complex synthesis techniques in a more facile and efficient way (i.e., at room temperature). This technique results in high quality ZnO nanocrystals of diameter 5–12 nm and different morphologies. Characterisation of ZnO products shows that both synthesis and ageing conditions have significant effects on the formation of the nanocrystals. Capping agents and ageing temperature/time can be used to control both size and crystallinity of the products. The use of *in situ* or *ex situ* ageing conditions can result in different particle morphologies. Both *in situ* and *ex situ* ageing shows that mild ageing conditions (e.g., 60–80°C and 24–48 hours) are required to produce the highest quality nanomaterials.

1. Introduction

ZnO semiconductor nanocrystals (NCs) are receiving much attention due to their novel optical [1–3] and electronic properties [4] and applications in solar cells [5, 6], light emitting diodes [7, 8] and catalysis [9]. Recent advances in charge transfer doping to make band gap variable nanocrystals [10–14] further enhance their potential as components of future nanotechnology. One of the key features in this system is the use of surface organic capping moieties which facilitate control of the unique properties which arise in the nanometre size scale regime.

A key ingredient for the study and applications of ZnO NCs is a reliable synthetic route to high-quality materials. While ZnO nanocrystals can be synthesized by a variety of methods, the most successful in terms of controlled size, size-dispersion and crystallinity has been the high-temperature decomposition of organometallic precursors in a coordinating solvent [15–17]. However, these methods usually require complex laboratory equipment and use expensive precursors. Experiments are strictly engineered by choice of ligands and solvents so that the zinc precursor complex is stable at low temperatures but unstable at higher leading to particle development. The solvents used must have relatively high boiling point and be inert to either the precursors or the products. Recently, there have been several reports of solution-phase synthesis of ZnO colloids at low temperature, mainly based on the hydrolysis of zinc salts [18–20] or zinc alkoxides [21, 22] (in organic solvents) and on electrochemical routes [23, 24]. The use of advanced engineered polymer templates [25–27] and reverse micelles [22, 28] have also been exploited in order to control both particle morphologies and sizes. However, unless extreme thermal treatments are applied after the synthesis, such preparative routes provide nanocrystalline ZnO with hydroxylated surfaces and/or organic molecules that can significantly affect material properties. This is important as surface-related defects account for both radiative and nonradiative decay channels competing with the ZnO band-edge emission [29], while surface-bound molecules [30, 31] or acid-basic sites can influence emission properties as well as redox potentials and interfacial electron-transfer rates [32].

Because of the limitations of the methodologies used thus far, there is a clear requirement to develop simple synthetic nonhydrolytic approaches coupled to the use of so-called capping ligands that coordinate to the surface and limit

growth whilst controlling surface chemistry (e.g., passivation of surface traps, particle dispersion in solvents, etc.). The goal of many studies is to provide a facile methodology, using common chemicals and laboratory apparatus to achieve size, shape, crystallinity and surface defect control by *in situ* synthesis and functionalization in a simple, cost-effective, and convenient way. The direct liquid phase precipitation (DLPP) strategy [33, 34] developed recently by us provides a facile, nonhydrolytic way to synthesize most binary or even ternary metal oxides at room temperature (RT). In this paper modification of this strategy is demonstrated for the synthesis of size monodispersed ZnO NCs at room temperature (RT). Compared with other low temperature solution phase approaches, DLPP can produce the ZnO NCs with higher quality in terms of shape-, size, crystallinity, and surface detect control whilst being a chemically convenient, efficient and energy saving (no calcination or heat input required) method to synthesise ZnO NCs in a readily scalable way.

2. Experimental

2.1. Materials. All chemicals are reagent grade and used asreceived. Na_2O (97%), $ZnCl_2$ (99%), oleic acid (OLA), methanol, and anhydrous ethanol were purchased from Aldrich. Hexadecylamine (HDA) was purchased from Fluka.

2.2. Synthesis of ZnO NCs. A typical synthesis consists of mixing of two prepared solutions. In solution 1, Na_2O and 2 mmol of hexadecylamine (the role of HDA is complex and discussed in detail below) was dissolved into 20 mL anhydrous ethanol to form a 0.1 M Na_2O solution. In solution 2, $ZnCl_2$ together with oleic acid (OLA) at fixed molar ratios indicated in the text was mixed in ethanol to yield a 0.1 M zinc cation solution. Solution 1 and 2 are combined under vigorously magnetic stirring at room temperature (RT) or as specified for 2 hours. On mixing, the solution becomes immediately turbid followed by the formation of white precipitate (nanocrystal aggregates). It is proposed that the DLPP method involves the direct reaction of O^{2-} anions with metal cations to yield the metal oxide [33, 34]. Under continued stirring the solution gradually becomes clearer (a little cloudy at RT but clearer at the elevated temperature, e.g., 60°C) as the as-formed "sticky" precipitate settles. The resulting white precipitate was aged *in situ* in the solution at 60–105°C for 24–188 h and the precipitate was collected by filtration (0.2 μm filter paper) and washed with ethanol and then acetone twice. For *ex situ* ageing, the filtrate was dispersed into 10 mL of toluene which results in rapid redispersion of the precipitate which was then reformed by the addition of 70 mL of methanol and the mixture was aged at 60°C for 10–120 hours. The precipitate was harvested and washed as described above. The typical ageing temperature, time, and oleic acid/Zn^{2+} ratio, unless otherwise stated, refer to 60°C, 24 hours, and 1 : 2, respectively, in this paper.

2.3. Analyses. The powder samples were analyzed by: a JEOL 2000FX transmission electron microscope (TEM) operating at 200 kV, a Phillips Xpert MPD X-ray diffractometer (XRD) using Cu Kα radiation at an anode voltage of 40 kV (with a high sensitivity X′Celerator detector) and a high performance AXIS 165 X-ray photoelectron spectrometer (XPS) using a pass energy of 20 eV. In addition, UV-vis (ultraviolet-visible) and photoluminescence spectra were recorded using a Cary 50 UV-visible spectrophotometer and a Perkin Elmer LS50B fluorescence spectrometer, respectively.

3. Results and Discussion

ZnO NCs are immediately formed upon the mixing of two portions of reactant solutions in the one-step synthesis. It should be noted that the products formed are weak aggregates of the nanocrystals but these can be rapidly dispersed in nonpolar solvents. Figure 1(a) shows the *in situ* ageing temperature has significant influence on the nanocrystal (NC) size (note the OLA/Zn^{2+} molar ratio = 1 : 2). ZnO NCs of 5 nm (using Scherrer formulism) are produced by synthesis at 60°C for 24 hours whilst the NC size increases to about 10 nm are produced when the ageing temperature is increased to 80°C. However, the increase of NC size with ageing temperature is complex (see Figure 1(d)) and crystal size is seen to decrease if the ageing temperature exceeds 100°C. Ageing time also affects the NC size and structure. The NCs grow from 7.5 nm to 10 nm, after the ageing time changes from 24 to 67 hours at 60°C as seen in Figure 1(b). However, this is a maximum size as the NC size decreases to about 6 nm on extended times (67 h). This is surprising as the maximum size of bare ZnO NCs formed in the absence of ligands is expected to be only determined by the metal cation concentration. It is suggested that this limited NC size results from competitive solution equilibria resulting from both the precipitation, and dissolution of ZnO species in ethanol. These solution equilibria arise from the presence of the strongly coordinating ligands. Carboxyl-containing long chain molecules have strong affinity to the ZnO matter due to the strong interaction between Zn^{2+} and carboxyl as they are coordinated in the form of zinc oleate and stearate salts [35, 36] and form a ligand passivation shell on the surface of ZnO NCs. The presence of OLA and HDA can be expected to lead to partially dissolution (etching) of the nanoparticles. Reactions to consider are the formation of soluble zinc oleate and the possibility of HDA-OLA reactions leading to stripping of a protective OLA layer. As might be expected, the NC size decreases with the increase of OLA/Zn^{2+} ratio as shown in Figure 1(c) and it can be verified that these ligands significantly inhibit the growth of the ZnO NCs.

The XRD data of the samples prepared with different OLA/Zn^{2+} ratio are apparently contradicted by TEM analysis. The micrographs shown in Figure 2 appear to indicate that the "nanocrystals" decrease in size with a decrease in the OLA/Zn^{2+} ratio. The average particle sizes measured by TEM are 11.31 (6.1), 4.85 (6.3), 4.88 (6.9) and 4.82 (7.9) nm (standard deviations given in brackets and all date

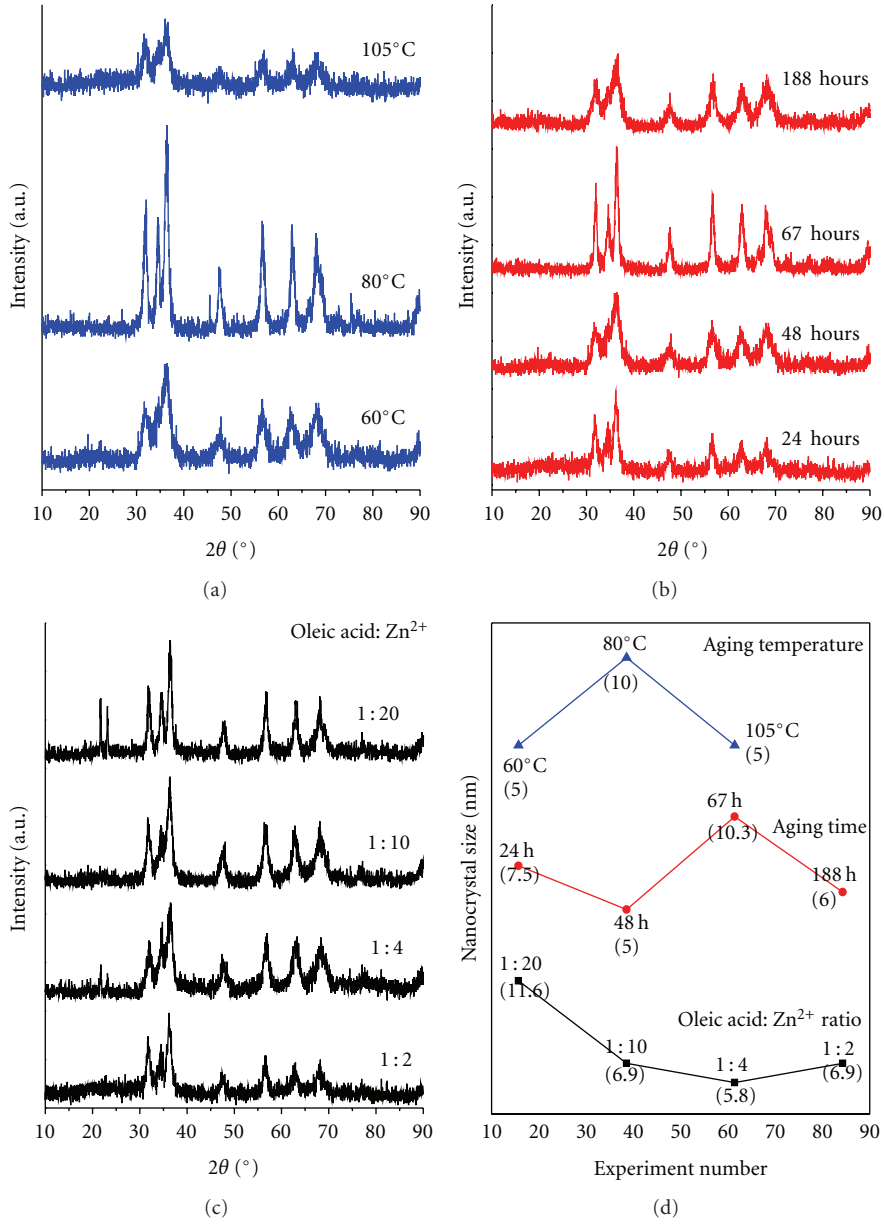

Figure 1: X-ray diffraction (XRD) patterns of the OLA-ZnO nanocrystals (NCs). (a) Aged in situ at different temperature for 48 hours with oleic acid/Zn^{2+} ratio of 1 : 2, (b) aged in situ at 60°C for different time oleic acid/Zn^{2+} ratio of 1 : 2, (c) aged in situ at 60°C for 24 hours with different oleic acid/Zn^{2+} ratio and (d) the nanocrystal size (shown in the parenthesis) under different ageing conditions calculated by Scherrer's equation.

are estimated from particle size distributions (PSDs) which are provided in the supporting information for all TEM data reported here) as the OLA/Zn^{2+} molar ratio decreases from 1 : 2, 1 : 4, 1 : 10, to 1 : 20, respectively. This contradiction between the characterisation methods can be attributed to the fact that synthesis results in the formation of individual particles consisting of a few aggregated nanocrystals or polycrystal grain structures which are observed by HRTEM (Figure 5(b)). XRD indicates the component nanocrystal size whilst TEM indicates the total particle size. It can be seen in the data that increasing OLA/Zn^{2+} ratio not only reduces the NC size but also improves the size dispersivity. This is probably related to the OLA preventing NC growth which improves size monodispersivity by limiting the growth process.

The complexity of effects resulting from changes in *in situ* ageing time and temperature revealed by XRD are also observed in the TEM data, as shown in Figures 3(a)–3(d). It was generally observed that particle size decreases on extended ageing at similar temperatures (but monodispersivity is improved as explained above). An example is shown in Figure 3(e) for 60°C ageing where the particle size changes from 6.1 to 4.7 nm after ageing at 48 and 188 h, respectively. The ageing temperature has a profound

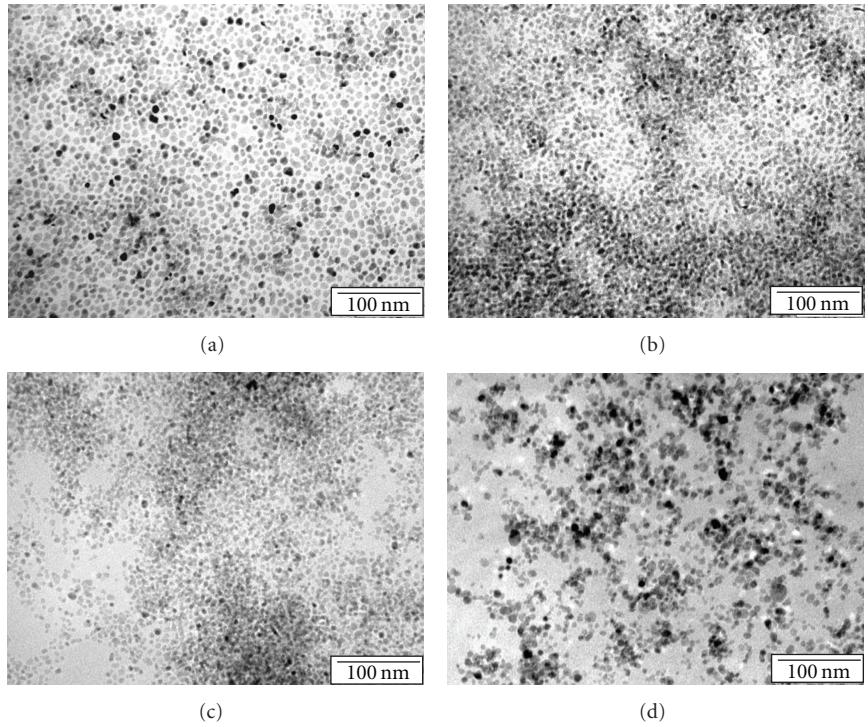

Figure 2: Transmission electron microscopy (TEM) images of the OLA-ZnO NCs synthesized by different molar ratio of oleic acid to Zn^{2+}: (a) 1 : 2; (b) 1 : 4; (c) 1 : 10 and (d) 1 : 20. All scale bars are 100 nm.

effect on the shape of the ZnO nanocrystals as revealed in Figures 3(a), 3(c), and 3(d). At 60°C ageing temperatures, the products are generally uniform in shape but at 80°C (Figure 3(c)) the crystals become elongated to rod-like structures. However, at higher age temperatures of 105°C more uniform particles are formed presumably because of ZnO solubility as described above. As seen by XRD, high ageing temperatures (105°C, NC size = 5.4 nm) result in a decrease in the size of the particles compared to lower temperatures (80°C, NC size = 8.6 nm). This decrease in the NC size can also be ascribed to the partial dissolution of the NCs as described above, since particle dissolution might be expected to become more important at high ageing temperature/time. The growth of particles at lower temperatures appears to result from an Ostwald ripening mechanism. If the reaction is carried out as usual (60°C) and stirred for two hours, subsequent addition of solid $ZnCl_2$ and Na_2O (stoichiometric amounts equivalent to those already present in solution) results in well-sized dispersed particles (Figure 3(f)) suggesting that the previously formed nanocrystals "consume" the newly formed smaller size materials efficiently and all ZnO NCs reach the same size provided that the ageing time is long enough. Understanding the high temperature behavior is probably related to the presence of HDA. Although it is commonly used in ZnO synthesis, its role of HDA is probably not as a simple surfactant (particle spacer) or surface complexing agent. Zhong and Knoll [37] have suggested that it controls particle morphology by determining the OLA interaction with the ZnO component. It was found here that HDA molecules cannot form stable HDA-ZnO complexes and almost all HDA molecules are removed from the product ZnO during precipitate washing with only trace nitrogen being observed by elemental analysis. On the basis of this work, we suggest that at reaction between HDA and OLA occurs at the highest age temperatures resulting in removal of the capping OLA ligands and so promoting ZnO dissolution as postulated earlier. Evidence for this assertion can be seen in Figures 4(a), 4(b), 4(c), and 4(d). Here, the *ex situ* ageing which results in HDA removal prior to ageing shows a simple variation of nanocrystal size with time. The NC size increases progressively from 6.8 to 12.1, 13.2, and 13.7 nm after ageing at 10, 24, 72, and 120 h. Extended ageing only results in a slow crystal growth, and this is related to decreasing solution concentration. As might be expected the polydispersity increases with age time (from a value of around 10 to 15 nm—see supporting information) and is consistent with the statistical nature of Ostwald ripening.

It should be noted that the OLA-ZnO NCs are highly dispersible and readily "soluble" in nonpolar solvents, for example, toluene, hexane, and chloroform, and the nanocrystal aggregates are reformed rapidly from the dispersed NCs in ethanolic and methanolic solutions. The term "soluble" is used as these solutions are clear because the dispersed particle size is well below that required for light scattering although evidence for small aggregates is present in UV-vis analysis (as detailed below). During growth the presence of these nonpolar solvents have dramatic effects of particle morphology. Figure 5(a) shows typical data from an *ex situ* ageing experiment carried out without addition of methanol

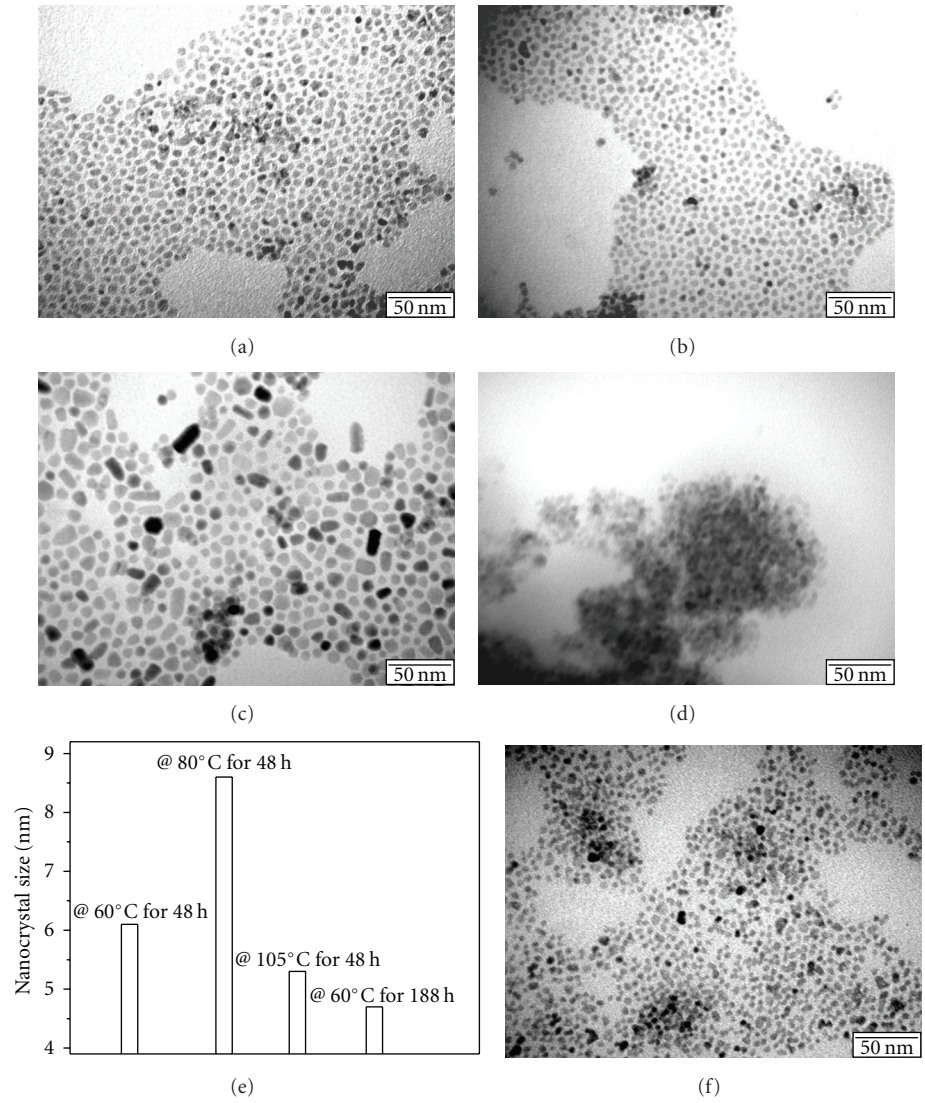

Figure 3: TEM images of the OLA-ZnO NCs obtained under different in situ ageing conditions: (a) 60°C for 48 hours; (b) 60°C for 188 hours; (c) 80°C for 48 hours; (d) 105°C for 48 hours and (e) the maximum mode of the nanocrystal size distribution from image (a)–(d); and (f) a sequential addition of metal cations where the reaction is initiated and run for two hours and additional stoichiometric amounts of Na_2O and $ZnCl_2$ solids are added during the extended ageing treatment (60°C for 188 hours). All scale bars are 50 nm.

(i.e., toluene only aged). Well-defined ZnO NCs where the crystals have flake-like polygonal shape; for example, rectangle, pentagon, and hexagon are formed. Lattice images can be observed by high resolution TEM as shown in Figure 5(b). The interspace distance between two adjacent white lines is 2.45 Å, and this is in agreement with the known spacing (1 0 1) planes of the zinc oxide (JCPDF no: 36-1451) structure (2.48 Å).

As well as the TEM and XRD analysis, spectroscopic evidence for the formation of ZnO nanocrystals is provided. UV-vis spectra (Figure 6(a)) of ZnO NCs (60°C for 188 h synthesis as described in Figure 3(b)) dispersed in hexane (following simple treatment in an ultrasonic bath) show a sharp peak at 230 nm (5.40 eV) and a steep slope centered at 361 nm (3.43 eV) and both these absorption energies are significantly higher than that of the bulk ZnO (3.3 eV). The sharp peak may be ascribed to the monodispersed ZnO NCs while the slope line corresponds to a UV absorbance caused by larger NC aggregates [38] that persist in solution. Figure 6(b) shows three obvious PL emission bands at 380 (3.26 eV), 421 (2.94 eV), and 520 nm (2.38 eV) and can be observed at two different photon excitation wavelengths (250 and 300 nm). The peak at 380 nm is attributed to the recombination though free exciton while the small peak at 421 nm is probably related to a deep-level carrier recombination [39]. However, the large broad feature centered at 520 nm corresponds to the defect-related emission [40].

An XPS survey spectrum of ZnO NCs (60°C for 188 h synthesis as described in Figure 3(b)) as shown in Figure 7(a) provides elemental analysis and is typical of the materials prepared here. All X-ray photoelectron peaks are identified

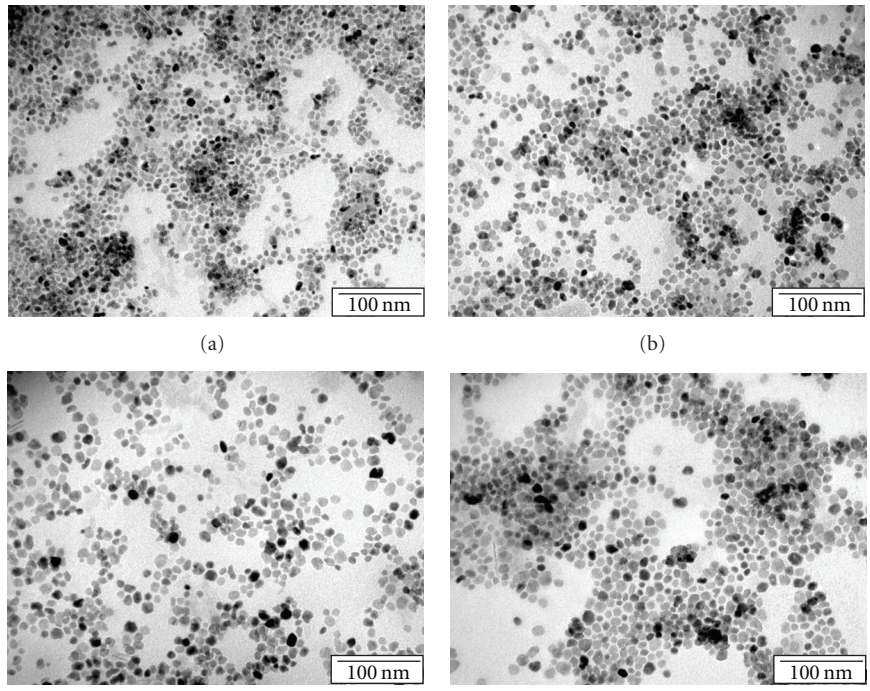

Figure 4: TEM images of the as-synthesized OLA-ZnO NCs aged ex situ at 60°C for different time: (a) 10, (b) 24, (c) 72, and (d) 120 hours. All scale bars are 100 nm.

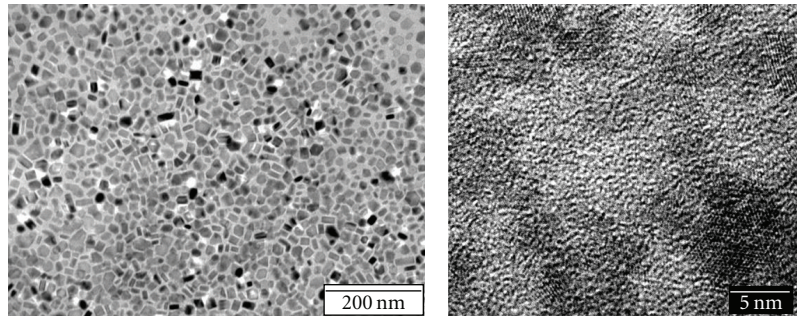

Figure 5: TEM images of the OLA-ZnO NCs synthesized at 60°C for 67 hours (a) and the corresponding high resolution TEM image (b).

in the figure and are consistent with the synthesis of carbon containing ZnO nanocrystals. Any unmarked peaks are from the complex set of Zn Auger features. There is a very weak contribution at 1070 eV due to Na (Na1s). The carbon (C1s peak position centered at 285.0 eV and typical of aliphatic carbon) is around 85% of the total photoelectron yield and is as expected for ZnO particles with dense outer ligand shells of oleic at the surface. Only trace nitrogen (N1s peak at 405 eV) is detected in the XPS spectra and this also conforms to the results obtained by the element analysis. The Zn2p and O1s signals are shown in high resolution form in Figure 7(b). The peak area ratio is consistent with the formation of ZnO and the binding energy positions (Zn2p3/2 = 1022 eV and O1s = 530 eV) are also typical of ZnO.

4. Conclusions

ZnO nanocrystals with a diameter of 5–12 nm have been successfully synthesized in a facile, quick, laboratory-friendly manner via one-step precipitation reaction of Zn^{2+} and O^{2-} species in nonaqueous solvents. The presence of both long-chain amine and oleic acid makes the synthesis controllable in terms of size, morphology, and crystallinity and highly solvent dispersible products are, therefore, synthesized. The results show that both the reaction conditions, for example, the OLA/Zn^{2+} ratio and the ageing conditions have profound effect on the nanocrystal size and dispersivity. The use of *in situ* or *ex situ* ageing conditions can also result in different particle morphologies. Both i*n situ* and *ex situ* ageing showing that mild ageing conditions (e.g., 60–80°C

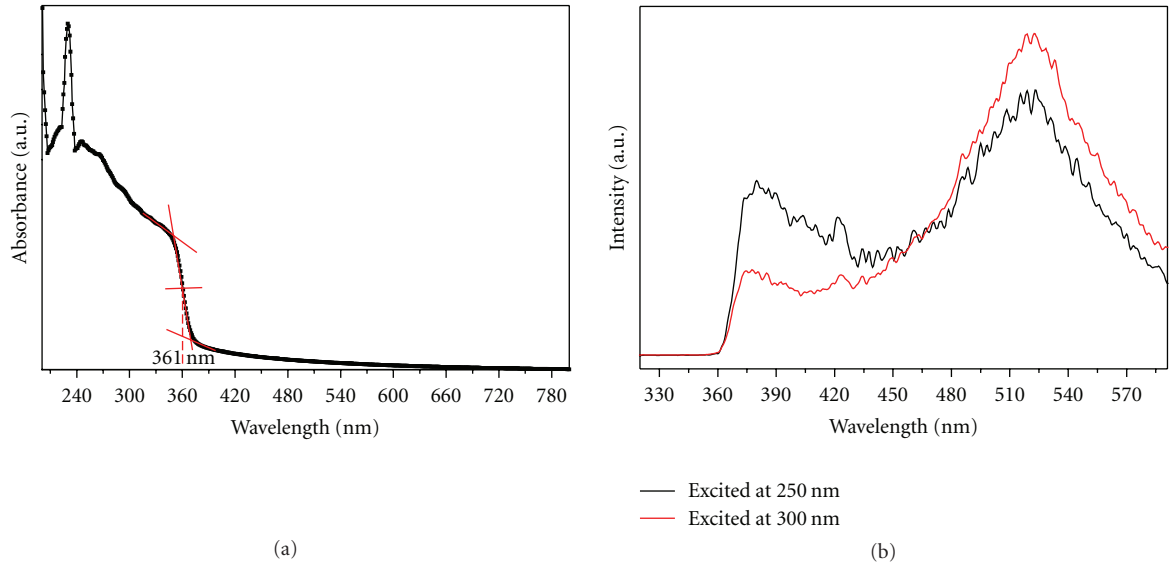

Figure 6: UV-vis absorbance spectrum (a) and photoluminescence (PL) emission spectra (b) of OLA-ZnO NCs (60°C for 188 h synthesis described in Figure 3(b) and text) dispersed in hexane.

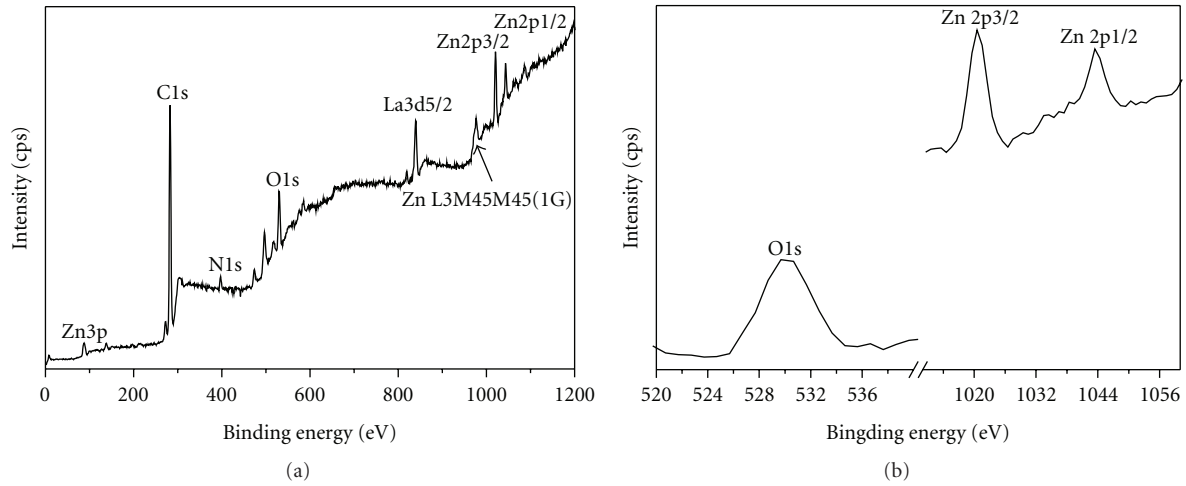

Figure 7: X-ray photoelectron (XPS) survey spectrum (a) of OLA-ZnO NCs (60°C for 188 h synthesis described in Figure 3(b) and text) and its detailed Zn and O element XPS spectrum (b).

and 24–48 hours) are required to produce the highest quality nanomaterials. Under the mild ageing conditions, a longer time, and higher temperature favour the formation of higher quality NCs while the effect is more complex when the precipitated nanomaterials is treated under harsher conditions. The OLA capped ZnO nanocrystals are stable and highly dispersible in most nonpolar solvents, where UV-vis absorbance features show a significant quantum size effect on the monodispersed ZnO NCs whilst PL emissions demonstrate both size- and defect-related energy processes.

Supporting Information Available

Particle size distributions (PSDs) data is available free of charge via the internet at http://www.hindawi.com/journals/jnm/.

Acknowledgment

The authors thank SFI (Science Foundation of Ireland) for the funding supports through the BIONANOINTERACT Strategic Research Cluster Grant 07/SRC/B1155.

References

[1] U. Banin and O. Millo, "Tunneling and optical spectroscopy of semiconductor nanocrystals," *Annual Review of Physical Chemistry*, vol. 54, pp. 465–492, 2003.

[2] J. Geng, B. Liu, L. Xu, F.-N. Hu, and J.-J. Zhu, "Facile route to Zn-based II-VI semiconductor spheres, hollow spheres, and core/shell nanocrystals and their optical properties," *Langmuir*, vol. 23, no. 20, pp. 10286–10293, 2007.

[3] P. E. Lippens and M. Lannoo, "Optical properties of II-VI semiconductor nanocrystals," *Semiconductor Science and Technology*, vol. 6, no. 9A, pp. A157–A160, 1991.

[4] R. Viswanatha, P. K. Santra, and D. D. Sarma, "Self assembly and electronic structure of ZnO nanocrystals," *Journal of Cluster Science*, vol. 20, no. 2, pp. 389–398, 2009.

[5] Q. Zhang, T. P. Chou, B. Russo, S. A. Jenekhe, and G. Cao, "Aggregation of ZnO nanocrystallites for high conversion efficiency in dye-sensitized solar cells," *Angewandte Chemie International Edition*, vol. 47, no. 13, pp. 2402–2406, 2008.

[6] J. Bouclé, H. J. Snaith, and N. C. Greenham, "Simple approach to hybrid polymer/porous metal oxide solar cells from solution-processed ZnO nanocrystals," *Journal of Physical Chemistry C*, vol. 114, no. 8, pp. 3664–3674, 2010.

[7] M. C. Newton, S. Firth, and P. A. Warburton, "Photoresponse of ZnO tetrapod nanocrystal Schottky diodes," *IEEE Transactions on Nanotechnology*, vol. 7, no. 1, pp. 20–23, 2008.

[8] E. Sun, F.-H. Su, Y.-T. Shih et al., "An efficient Si light-emitting diode based on an n- ZnO/SiO_2-Si nanocrystals-SiO_2/p-Si heterostructure," *Nanotechnology*, vol. 20, no. 44, Article ID 445202, 2009.

[9] M. L. Kantam, K. B. S. Kumar, and Ch. Sridhar, "Nanocrystalline ZnO as an efficient heterogeneous catalyst for the synthesis of 5-substituted 1*H*-tetrazoles," *Advanced Synthesis and Catalysis*, vol. 347, no. 9, pp. 1212–1214, 2005.

[10] A. S. Pereira, M. Peres, M. J. Soares et al., "Synthesis, surface modification and optical properties of Tb^{3+}-doped ZnO nanocrystals," *Nanotechnology*, vol. 17, no. 3, pp. 834–839, 2006.

[11] Y. S. Wang, P. J. Thomas, and P. O'Brien, "Optical properties of ZnO nanocrystals doped with Cd, Mg, Mn, and Fe ions," *Journal of Physical Chemistry B*, vol. 110, no. 43, pp. 21412–21415, 2006.

[12] M. Peres, A. Cruz, S. Pereira et al., "Optical studies of ZnO nanocrystals doped with Eu^{3+} ions," *Applied Physics A*, vol. 88, no. 1, pp. 129–133, 2007.

[13] Y. Liu, W. Luo, R. Li, H. Zhu, and X. Chen, "Near-infrared luminescence of Nd^{3+} and Tm^{3+} ions doped ZnO nanocrystals," *Optics Express*, vol. 17, no. 12, pp. 9748–9753, 2009.

[14] Y. S. Liu, W. Q. Luo, R. F. Li, and X. Y. Chen, "Optical properties of Nd^{3+} ion-doped ZnO nanocrystals," *Journal of Nanoscience and Nanotechnology*, vol. 10, no. 3, pp. 1871–1876, 2010.

[15] M. Epifani, J. Arbiol, R. Díaz, M. J. Perálvarez, P. Siciliano, and J. R. Morante, "Synthesis of SnO2 and ZnO colloidal nanocrystals from the decomposition of Tin(II) 2-ethylhexanoate and Zinc(II) 2-ethylhexanoate," *Chemistry of Materials*, vol. 17, no. 25, pp. 6468–6472, 2005.

[16] Y. C. Zhang, X. Wu, X. Y. Hu, and R. Guo, "Low-temperature synthesis of nanocrystalline ZnO by thermal decomposition of a "green" single-source inorganic precursor in air," *Journal of Crystal Growth*, vol. 280, no. 1-2, pp. 250–254, 2005.

[17] S. Labuayai, V. Promarak, and S. Maensiri, "Synthesis and optical properties of nanocrystalline ZnO powders prepared by a direct thermal decomposition route," *Applied Physics A*, vol. 94, no. 4, pp. 755–761, 2009.

[18] L. Spanhel and M. A. Anderson, "Semiconductor clusters in the sol-gel process: quantized aggregation, gelation, and crystal growth in concentrated ZnO colloids," *Journal of the American Chemical Society*, vol. 113, no. 8, pp. 2826–2833, 1991.

[19] E. A. Meulenkamp, "Synthesis and growth of ZnO nanoparticles," *Journal of Physical Chemistry B*, vol. 102, no. 29, pp. 5566–5572, 1998.

[20] E. M. Wong, J. E. Bonevich, and P. C. Searson, "Growth kinetics of nanocrystalline ZnO particles from colloidal suspensions," *Journal of Physical Chemistry B*, vol. 102, no. 40, pp. 7770–7775, 1998.

[21] C. L. Carnes and K. J. Klabunde, "Synthesis, isolation, and chemical reactivity studies of nanocrystalline zinc oxide," *Langmuir*, vol. 16, no. 8, pp. 3764–3772, 2000.

[22] D. Kaneko, H. Shouji, T. Kawai, and K. Kon-No, "Synthesis of ZnO particles by ammonia-catalyzed hydrolysis of zinc dibutoxide in nonionic reversed micelles," *Langmuir*, vol. 16, no. 9, pp. 4086–4089, 2000.

[23] R. M. Nyffenegger, B. Craft, M. Shaaban, S. Gorer, G. Erley, and R. M. Penner, "A hybrid electrochemical/chemical synthesis of zinc oxide nanoparticles and optically intrinsic thin films," *Chemistry of Materials*, vol. 10, no. 4, pp. 1120–1129, 1998.

[24] S. Mahamuni, K. Borgohain, B. S. Bendre, V. J. Leppert, and S. H. Risbud, "Spectroscopic and structural characterization of electrochemically grown ZnO quantum dots," *Journal of Applied Physics*, vol. 85, no. 5, pp. 2861–2865, 1999.

[25] L. Guo, S. Yang, C. Yang et al., "Synthesis and characterization of poly(vinylpyrrolidone)-modified zinc oxide nanoparticles," *Chemistry of Materials*, vol. 12, no. 8, pp. 2268–2274, 2000.

[26] A. Taubert, G. Glasser, and D. Palms, "Kinetics and particle formation mechanism of zinc oxide particles in polymer-controlled precipitation from aqueous solution," *Langmuir*, vol. 18, no. 11, pp. 4488–4494, 2002.

[27] A. Taubert, D. Palms, Ö. Weiss, M.-T. Piccini, and D. N. Batchelder, "Polymer-assisted control of particle morphology and particle size of zinc oxide precipitated from aqueous solution," *Chemistry of Materials*, vol. 14, no. 6, pp. 2594–2601, 2002.

[28] B. S. Zou, V. V. Volkov, and Z. L. Wang, "Optical properties of amorphous ZnO, CdO, and PbO nanoclusters in solution," *Chemistry of Materials*, vol. 11, no. 11, pp. 3037–3043, 1999.

[29] A. van Dijken, E. A. Meulenkamp, D. Vanmaekelbergh, and A. Meijerink, "The kinetics of the radiative and nonradiative processes in nanocrystalline Zno particles upon photoexcitation," *Journal of Physical Chemistry B*, vol. 104, no. 8, pp. 1715–1723, 2000.

[30] S. Monticone, R. Tufeu, and A. V. Kanaev, "Complex nature of the UV and visible fluorescence of colloidal ZnO nanoparticles," *Journal of Physical Chemistry B*, vol. 102, no. 16, pp. 2854–2862, 1998.

[31] S. Sakohara, M. Ishida, and M. A. Anderson, "Visible luminescence and surface properties of nanosized ZnO colloids prepared by hydrolyzing zinc acetate," *Journal of Physical Chemistry B*, vol. 102, no. 50, pp. 10169–10175, 1998.

[32] M. Che, C. Naccache, and B. Imelik, "Electron spin resonance studies on titanium dioxide and magnesium oxide-Electron donor properties," *Journal of Catalysis*, vol. 24, no. 2, pp. 328–335, 1972.

[33] L. Chen, J. Xu, D. A. Tanner et al., "One-step synthesis of stoichiometrically defined metal oxide nanoparticles at room

temperature," *Chemistry: A European Journal*, vol. 15, no. 2, pp. 440–448, 2009.

[34] L. Chen, J. Xu, J. D. Holmes, and M. A. Morris, "A facile route to ZnO nanoparticle superlattices: synthesis, functionalization, and self-assembly," *Journal of Physical Chemistry C*, vol. 114, no. 5, pp. 2003–2011, 2010.

[35] W. S. Chiu, P. S. Khiew, D. Isa et al., "Synthesis of two-dimensional ZnO nanopellets by pyrolysis of zinc oleate," *Chemical Engineering Journal*, vol. 142, no. 3, pp. 337–343, 2008.

[36] C. Li, Y. Li, Y. Wu, B. S. Ong, and R. O. Loutfy, "Synthesis of zinc oxide nanocrystals by thermal decomposition of Zn-oleate in organic medium," *Science in China Series E*, vol. 51, no. 12, pp. 2075–2079, 2008.

[37] X. Zhong and W. Knoll, "Morphology-controlled large-scale synthesis of ZnO nanocrystals from bulk ZnO," *Chemical Communications*, no. 9, pp. 1158–1160, 2005.

[38] C. V. Santilli, S. H. Pulcinelli, M. S. Tokumoto, and V. Briois, "In situ UV-vis and EXAFS studies of ZnO quantum-sized nanocrystals and Zn-HDS formations from sol-gel route," *Journal of the European Ceramic Society*, vol. 27, no. 13–15, pp. 3691–3695, 2007.

[39] C. P. Chen, M. Y. Ke, C. C. Liu, Y. J. Chang, F. H. Yang, and J. J. Huang, "Observation of 394 nm electroluminescence from low-temperature sputtered n-ZnO/SiO_2 thin films on top of the *p*-GaN heterostructure," *Applied Physics Letters*, vol. 91, no. 9, Article ID 091107, 2007.

[40] S. Chakrabarti, D. Ganguli, and S. Chaudhuri, "Photoluminescence of ZnO nanocrystallines confined in sol-gel silica matrix," *Journal of Physics D*, vol. 36, no. 2, pp. 146–151, 2003.